第36卷第5期
2017年10月

红外与毫米波学报
J. Infrared Millim. Waves

Vol. 36, No. 5
October, 2017

文章编号: 1001 - 9014(2017)05 - 0563 - 07

DOI:10.11972/j.issn.1001 - 9014.2017.05.009

Surface micro-machined beam-steering antenna array for 60 GHz radios

ZHU Hua[1,2], LI Xiu-Ping[1,2*], FENG Wei-Wei[1,2], YAO Li[1,2], XIAO Jun[1,2], TIAN Yang[3], WANG Hong[3]

(1. School of Electronic Engineering, University of Posts and Telecommunications, Beijing 100876, China;
2. Beijing Key Laboratory of Work Safety Intelligent Monitoring,
Beijing University of Posts and Telecommunications, 100876 Beijing, China;
3. School of Electrical and Electronic Engineering, Nanyang Technological University, Singapore 639798, Singapore)

Abstract: A beam-steering antenna array based on surface micro-machined process was proposed for 60GHz high data rate wireless communication. The air-filled coaxial structure based surface micro-machined process provides low loss rectangular micro-coaxial transmission line and feeding network. The insertion loss of designed transmission line is less than 0.18dB for both measured and simulated results. Simulated and measured results agree well. The size of beam-steering antenna array is $17.5 \times 14.5 \times 0.42$ mm^3 and bandwidth is around 10 GHz (55 ~ 65 GHz) under the condition of voltage standing wave ratio (VSWR) less than 2, which covers full frequency band standard. The steering beam directions are ±35° with 11.8dBi and ±11° with 12.1 dBi at 60 GHz, respectively.

Key words: beam-steering antenna array, rectangular micro-coaxial transmission line, Butler matrix, low loss
PACS: 84.40.Ba, 84.40.Az, 84.35. +i, 02.10.Yn

基于微机械工艺的60 GHz波束扫描天线阵

朱 华[1,2], 李秀萍[1,2*], 冯魏巍[1,2], 要 栗[1,2], 肖 军[1,2], 田 阳[3], 汪 宏[3]

(1. 北京邮电大学电子工程学院,北京 100876;
2. 北京安全生产智能监控北京市重点实验室,北京 100876;
3. 新加坡南洋理工大学,新加坡 639798)

摘要:提出了一种应用于高速率无线通信的基于微机械工艺的波束扫描天线阵.基于微机械工艺的空气填充的同轴线结构能提供低损耗的矩形微同轴传输线和馈电网络设计.设计的传输线仿真和测试插入损耗均小于0.18 dB.仿真和测试结果吻合良好.波束扫描天线阵的尺寸为$17.5 \times 14.5 \times 0.42$ mm^3, -10 dB带宽为10 GHz(55 ~ 65 GHz),其带宽覆盖60 GHz标准的全频段.波束扫描角度分别为±35°和±11°.在60 GHz中心频点,增益分别为11.8 dBi和12.1 dBi.

关 键 词:波束扫描天线阵;矩形微同轴传输线;巴特勒矩阵;低损耗

中图分类号:TN827 + .3 **文献标识码**:A

Introduction

Recently, the unlicensed 60 GHz spectrum ranging from 57 to 66 GHz has been targeted for short-rang, high data rate (multiple Gb/s) communication. This band is attractive for a number of reasons, including the amount of spectrum available (7 GHz), suitability for frequency reuse, and high FCC the equivalent isotropic radiated power (EIRP) limit (40 dBm)[1]. The main limitations associated with the 60 GHz frequency range are antenna design and circuit integration problem, limited wall penetration, and high losses including oxygen absorption, high surface wave loss. Efficient, broadband and high-gain beamforming antennas are key performance. To be commercially viable, antenna solution must provide low cost, small size, and simple integration with 60 GHz radios.

At millimeter-wave frequencies, surface wave excitation leads to poor radiation efficiency, narrower band-

Received date: 2017-02-16, **revised date**: 2017-07-02 **收稿日期**:2017-02-16, **修回日期**:2017-07-02
Foundation items: Supported by the National Natural Science Foundation of China (61372036, 61601050); the project (6140135010116DZ08001, 6140518040116DZ02001)
Biography: ZHU Hua (1983-), female, Guilin, doctor. Research area involves millimeter wave and terahertz antenna array. E-mail: judy-cool@163.com
* **Corresponding author**: E-mail: xpli@bupt.edu.cn

width, degraded radiation patterns and undesired coupling between the various elements in array configurations. Surface waves reduction is challenge in mm-wave antenna design. There have been quite a few reported methods on how to reduce surface wave. Microelectromechanical systems (MEMS) is to reduce the thickness of the substrate locally under the antenna to obtain decreased dielectric permittivity [2]. Another method is to remove the semiconductor underneath the antenna to produce a cavity[3]. However, these processes are complex. Substrate integrated waveguide (SIW) has the advantages of low insertion loss and high power capability[4]. However, the SIW antenna has shortcomings of large size and narrow band. Recently, micro-machined millimeter-wave antennas become an attractive alternative as to conventional planner antennas due to 3D structure introducing low dielectric loss[5].

For short-range indoor communications, the link between transmitter and receiver can be shadowed because of human body interposition. Beam steering antenna array is one of solutions to solve this problem. By controlling phase shifter of the antennas, the radiated energy can be concentrated in a specific angle to avoid obstacles. A number of electronically steering antennas for this application have been proposed, including switched beam array[6], mechanically steering antennas[7], phased arrays[8] and MIMO antenna array[9]. The antenna array was composed of four pyramidal horns and four MMIC switches to achieve gain of 15.3 dBi and cover 120° areas, but the size was large[6]. Steerable beam antenna was composed by a dielectric lens which allowed steering mechanically the beam in elevation and azimuth[7]. The gain was up to 21 dBi and beam was from -45° to 45° for all azimuths. However, processing was complex. Two-dimensionally (2-D) scanning array employing a planar switched beam network (SBN) was proposed for 60 GHz[8]. Due to the use of PCB process, the loss was large. 2×2 MIMO antenna array based on microstrip patch arrays was proposed for 60 GHz applications[9]. Due to the non-correlation between MIMO antennas, the size was large.

In this paper, the rectangular micro-coaxial transmission line with lower insertion loss is proposed to overcome the surface wave loss in millimeter wave. The beam-steering antenna array was designed by surface micro-machined process. The beam-steering antenna array consists of three main parts: 1×4 antenna array, 4×4 butler matrix and transition. The cavity-backed circular patch antenna was designed for high gain and wide bandwidth. A4×4 Butler Matrix based on rectangular micro-coaxial transmission line is used to provide beam steering capability of forming four fixed beams covering 70° areas.

1 Rectangular micro-coaxial transmission line for low loss

Planar transmission lines, namely microstrip line (MS), coplanar waveguide (CPW) and grounded coplanar waveguide (GCPW), have provided flexibility in millimeter wave integrated circuit designs for decades. However, there are some drawbacks that degrade the performance of the designed circuits, such as parasitic coupling and radiation, increased ohmic coupling, dielectric losses and dispersion.

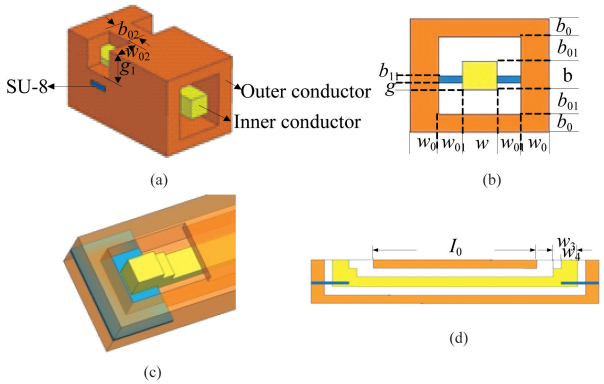

Fig. 1 Schematic of unit section of the rectangular micro-coaxial transmission line (a) 3D view (b) front view (c) pad (d) side view
图1 矩形微同轴传输线的示意图 (a) 3D 视图 (b)正视图 (c)焊盘 (d)侧视图

The rectangular micro-coaxial transmission line was designed for low loss and small size, as shown in Fig. 1. The designed rectangular micro-coaxial transmission line consists of inner conductor, outer conductor and SU-8 film. A thin SU-8 film is used as the dielectric support of inner conductor which shows excellent mechanical strength. The photoresist is applied as sacrificed layers for forming the air-filled coaxial structure. The hole on the outer conductor is used for etching the photoresist. To test the microwave performance of devices, pad is used to connect the device and probes. However, the planar pad is not compatible with the rectangular coaxial structure. The pad was designed with the signal line part supported by SU-8 film, as shown in Fig. 1(c). The cross sectional dimension of pad is exactly the same as the rectangular micro-coaxial transmission line.

The characteristic impedance of a transmission line can be calculated as[11]

$$Z_0 = \sqrt{\frac{L_{\text{len}}}{C_{\text{len}}}} = \frac{1}{v_{\text{p}} C_{\text{len}}} \quad , \quad (1)$$

where $v_{\text{p}} = 3 \times 108$ m/s is the phase velocity of the line, which is equal to the speed of light in vacuum for an air core TEM transmission line, and C_{len} is the capacitance per unit length of the transmission line.

For rectangular micro-coaxial transmission line where the width and thickness is larger than the gaps ($w > w_0, b > b_0$), the capacitance is calculated as[12]:

$$\begin{aligned} C_{\text{len}} &= 2\varepsilon\left(\frac{w}{b_0} + \frac{b}{w_0}\right) \\ &+ \frac{4\varepsilon}{\pi}\left[\ln\left(\frac{w_0^2 + b_0^2}{4b_0^2}\right) + 2\frac{b_0}{w_0}\arctan\left(\frac{b_0}{w_0}\right)\right] \\ &+ \frac{4\varepsilon}{\pi}\left[\ln\left(\frac{w_0^2 + b_0^2}{4b_0^2}\right) + 2\frac{w_0}{b_0}\arctan\left(\frac{w_0}{b_0}\right)\right] \quad . (2) \\ \varepsilon &= \varepsilon_0 = 8.85 \text{ pF/m} \end{aligned}$$

The characteristic impedance and the first high-order mode cut-off frequency are the key parameters of rectangular micro-coaxial transmission. As required by the

process, the thickness of each layer must be consistent ($b = b_0 = b_{01}$). The size is shown in Table 1. The proposed micro-coaxial transmission line was fabricated by in-house micro-machining process. The photograph is shown in Fig. 2. The length of the designed rectangular micro-coaxial transmission line is 4.7 mm.

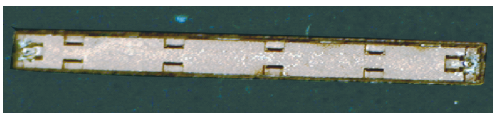

Fig. 2　Photographs of the fabricated micro-coaxial transmission line for 60 GHz
图 2　60 GHz 矩形微同轴传输线加工实物图

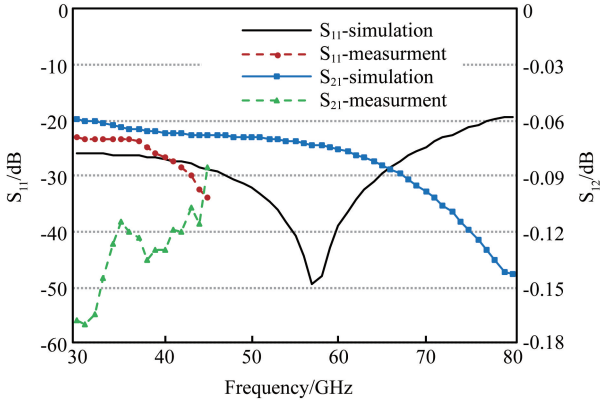

Fig. 3　Simulated and measured S-parameter of the micro-coaxial transmission line
图 3　矩形微同轴传输线的仿真和测量 S 参数

Simulated S_{11} is less than −10 dB cover 30 GHz to 80 GHz. Simulated insertion loss is less than 0.15 dB up to 80 GHz. The measurement is only up to 45 GHz due to the test conditions limitation. Measured insertion loss is less than 0.18 dB up to 45 GHz, as shown in Fig. 3. Simulated and measured results agree well.

Other three types of planar transmission lines (MS, CPW and GCPW) were designed and fabricated in 0.13 μm CMOS processes, as shown in Fig. 4. The length of the three transmission lines is 500 μm. The device information of three transmission lines is summarized in Table 2.

Table 2　Parameter of three transmission line (unit: μm)
表 2　其他三种传输线的参数(单位: μm)

Parameters	w_{11}	w_{12}	w_{13}	g_{12}	g_{13}	l_{11}
Value	7.2	10	8	5.6	15	500

Simulated and measured S_{11} of three transmission lines are less than -10 dB covering 30 to 45 GHz, as shown in Figs. 5(a-b). It is observed that insertion loss of CPW is less than other transmission lines.

The propagation constant (γ) of the transmission

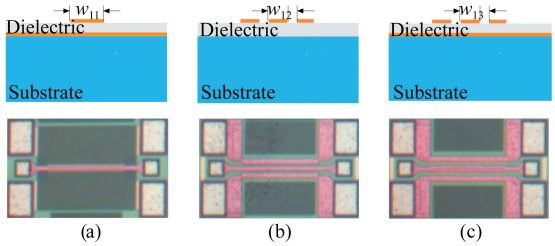

Fig. 4　Cross-section and Close-up chip photo of the transmission line. (a) MS, (b) CPW, (c) GCPW
图 4　三种在片传输线的截面图和特写图 (a) MS, (b) CPW, (c) GCPW

line can be determined from the S-parameters by[13]

$$G = \frac{1 - S_{11}^2 + S_{21}^2}{\sqrt{[(1 + S_{11})^2 - S_{21}^2][(1 - S_{11})^2 - S_{21}^2]}}, \quad (3)$$

$$\gamma = -\frac{1}{2l_{11}}\log\left|\frac{G-1}{G+1}\right|, \quad (4)$$

where l_{11} is the signal line effective length of the transmission line. The attenuation constant (α) and the phase constant (β) of the transmission line can be extracted from γ as

$$\gamma = \alpha + j\beta. \quad (5)$$

From Fig. 5(c), we can see the attenuation constant of the micro-coaxial transmission line is less than 0.01 dB/mm up to 45 GHz, which is the lowest in the three transmission lines.

2　Beam-steering antenna array design

The proposed beam-steering antenna array is integrated with 1×4 cavity-backed circular patch antenna array, 4×4 butler matrix and ceramic thin-film circuit, as shown in Fig. 6. The beam-steering function can be achieved by adaptively controlling the phase excitation of individual antenna elements. A 4×4 Butler Matrix based on rectangular micro-coaxial transmission line is used to provide the different phase differences. The transition structure of rectangular micro-coaxial to microstrip line was designed for minimum transmission loss and impedance matching for integration.

2.1　Cavity-backed circular patch antenna design

Surface micro-machined cavity-backed circular patch antenna was designed, as shown in Fig. 8. It consists of a circular patch, ladder probe, a backed cavity and three shorting pins. Due to the limitation of surface micro-machined process, the height of antenna is only 420 μm, which affects the bandwidth performance of antenna. The ladder probe was designed to enhance bandwidth. The three shorting pins are designed for supporting circular patch. The back cavity was designed for enhance the gain of antenna. The optimized dimensions of the antenna element are shown in Table 3. The simulated

Table 1　Parameters of rectangular micro-coaxial transmission line for 50 Ω characteristic impedance
表 1　50 Ω 特性阻抗的矩形微同轴传输线参数

Parameters	b	b_0	b_1	w	w_{01}	w_{02}	w_{03}	w_{04}	g	g_1	b_{11}	b_{02}	l_0
Value/μm	80	80	80	100	68	80	100	100	20	118	20	150	4 700

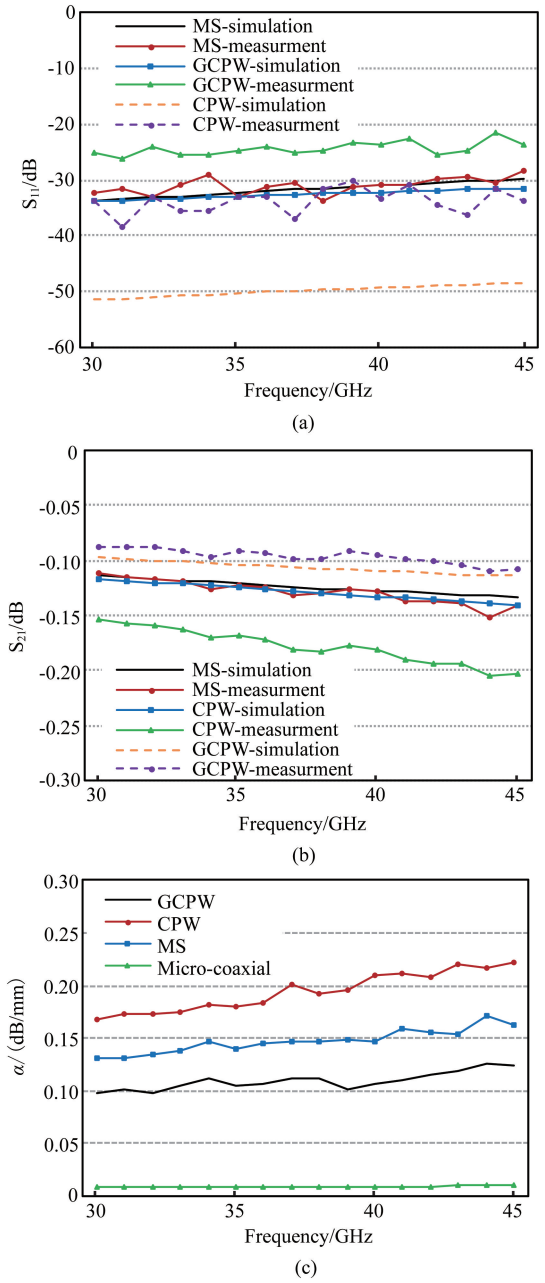

Fig. 5 Simulated and measured S-parameter of the transmission lines (a) S_{11} (b) S_{21} (c) Extracted attenuation per millimeter

图5 三种传输线的仿真和测量S参数 (a) S_{11} (b) S_{21} (c) 每毫米的衰减

results are shown in Fig. 8. It is observed that the bandwidth is 9.8 GHz (58 ~ 67.8 GHz) under the condition of S_{11} less than -10 dB. The gain of the antenna is 7.45 dBi at 60 GHz.

Table 3 Parameters of the antenna element

图3 天线阵的参数

Parameters	l	l_1	l_2	w_1	w_2	h	h_1
Value/μm	3 500	3 000	300	400	3 000	316	420
Parameters	b	b_1	b_2	R	d_1	d_2	d_3
Value/μm	8 100	100	580	2 160	1 120	1 700	650

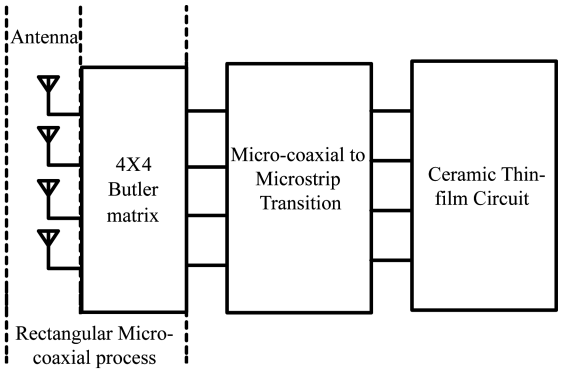

Fig. 6 The block diagram of beam-steering antenna array

图6 波束扫描天线的框图

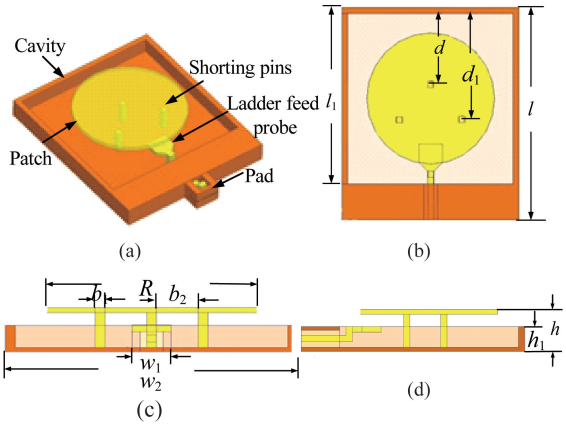

Fig. 7 The cavity-backed patch antenna structure (a) 3D view, (b) top view, (c) front view, (d) side view

图7 背腔天线的结构 (a) 3D 视图,(b) 俯视图,(c) 正视图,(d) 侧视图

2.2 Bulter matrix design

A 4 ×4 Butler matrix mainly consists of four 90° hybrid couplers, two 45° phase shifters and two cross-over structures, as shown in Fig. 9. The optimized dimensions of Butler matrix are shown in Table 4. Simulated S-parameters and phase differences of the Butler matrix network are shown in Fig. 10. S_{11} is less than −10 dB around 56 ~ 65 GHz. When Port 1 is excited, power distribution of outputs is within −6.3 ±0.8 dB. The phase differences between different output ports are −45° ±5.4°, 45° ±5°, −135° ±8°, 135° ±8°, respectively, over the frequency range. The Butler matrix designed by rectangular micro-coaxial transmission line achieves low loss and different phase differences to ensure the antenna array of different beam steering.

Table 4 Parameters of the Butler matrix

表4 巴特勒矩阵参数

Parameters	w_3	w_4	w_5	l_3	l_4	l_5	l_6	l_7	l_8
Value/μm	126	95	206	1 176	1 126	1 206	590	2 799.5	648

2.3 Rectangular micro-coaxial to microstrip transition design

The transition structure of rectangular micro-coaxial

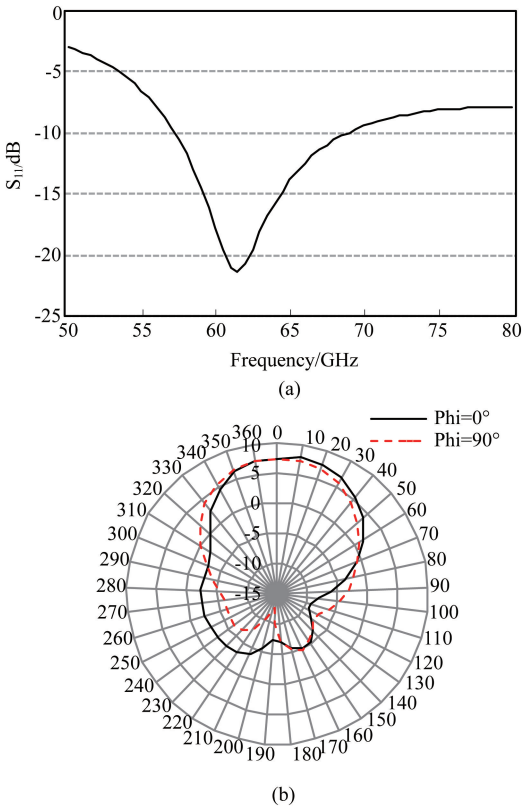

Fig. 8　Character parameter of element (a) S_{11}, (b) Radiation Pattern at 60 GHz
图 8　单元的参数 (a) S_{11}, (b) 60 GHz 的方向图

to microstrip line was designed. As shown in Fig. 11, a copper cylinder and via hole are used to connect the inner conductor of rectangular micro-coaxial to the conductor of the microstrip. A square slot is cut in the ground plane of the microstrip to separate via hole to the ground plane. The size of the slot is the same as the cross section of micro-coaxial cavity. A compensation structure was designed to reduce the parasitic inductance through the copper cylinder and via. The size is shown in Table V. Simulated result of S-parameter is shown in Fig. 12. It is obvious that the S_{11} is less than −10 dB cross the frequency band of 55 ~ 65 GHz. The insertion loss is less than 0.45 dB.

Table 5　Parameters of the transmission structure
表 5　转换结构的参数

Parameters	h_3	w_6	w_7	w_8	l_9	l_{10}	l_{11}
Value/μm	127	140	120	123	140	363	265

3　Results and discussions

A beam-steering antenna array based on surface micro-machined process is shown in Fig. 13. Antenna array and 4 × 4 Butler matrix is integrated in copper Substrate. Ceramic substrate connects with rectangular micro-coaxial through the transition structure. The ceramic thin-film circuit is assembled on single layer ceramic substrate

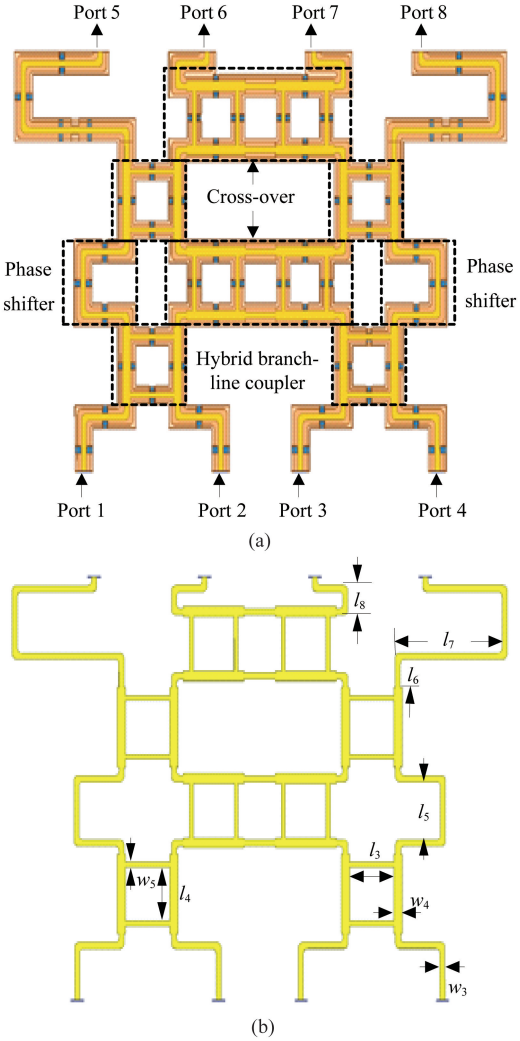

Fig. 9　Layout of designed 4 × 4 Butler matrix network: (a) schematic of the Bulter matrix, (b) inner of the Bulter matrix
图 9　4 × 4 的巴特勒矩阵的网络框图:(a) 巴特勒矩阵的示意图,(b) 巴特勒矩阵的内径

with 127 μm-thichness. The size is 17.5 × 14.5 × 0.42 mm^3.

It is observed that the bandwidth is 10 GHz (55 ~ 65 GHz) under the condition of VSWR less than 2, which includes worldwide unlicensed band, as shown in Fig. 14 (a). Simulated scanning radiation patterns in the −35°, −11°, 11°, 35° directions are shown in Fig. 14 (b). The antenna array is capable of scanning beams up to ±35° with 11.8 dBi and ±11° with 12.1 dBi at 60 GHz, respectively. The half-power beam width is 33° at the ±11° scanning beam, while it is 38° at the ±35° scanning beam.

The characteristics of the proposed antenna are compared with previous works of beam-steering antenna array in Table 6. A comparison between the SIW slot antenna array, printed circuit board (PCB) antenna array and proposed antenna was made for the similar feeding networks. It is seen that notable features of the proposed antenna array are small size and wide bandwidth and low insertion loss of feeding network.

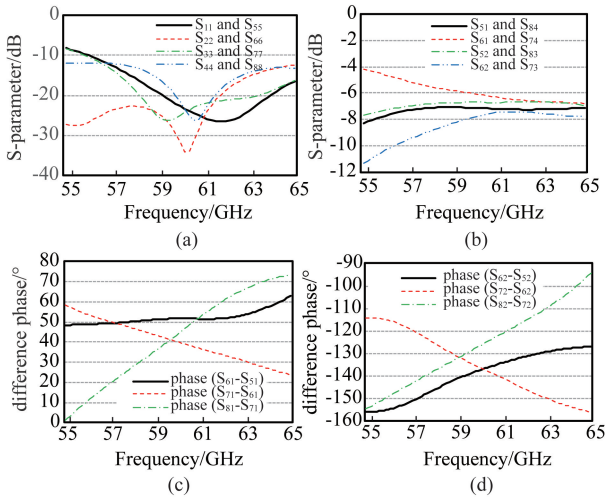

Fig. 10 Simulated S-parameter and phase difference of Butler matrix (a) $S_{11}/S_{22}/S_{33}/S_{44}/S_{55}/S_{66}/S_{77}$ (b) $S_{51}/S_{61}/S_{71}/S_{81}/S_{52}/S_{62}/S_{73}/S_{83}$ (c) Phase difference of port1 to other ports (d) Phase difference of port2 to other ports

图 10 巴特勒矩阵的仿真 S 参数和相位差 (a) $S_{11}/S_{22}/S_{33}/S_{44}/S_{55}/S_{66}/S_{77}$ (b) $S_{51}/S_{61}/S_{71}/S_{81}/S_{52}/S_{62}/S_{73}/S_{83}$ (c) 1 端口与其他端口的相位差 (d) 2 端口与其他端口的相位差

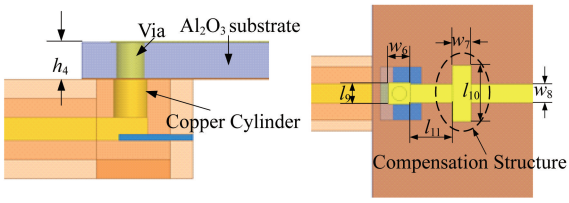

Fig. 11 Micro-coaxial to microstrip transition structure. (a) Side view, (b) top view

图 11 矩阵微同轴传输线与微带线的转换结构 (a) 侧视图 (b) 俯视图

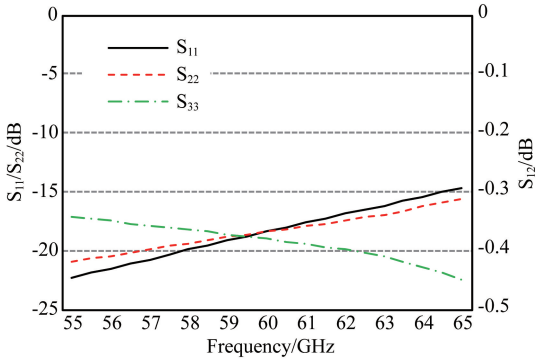

Fig. 12 Simulated S-parameter of the micro-coaxial to microstrip transition structure

图 12 矩形微同轴到微带线转换结构的 S 参数

Table 6 Key Date of Several 60 GHz Antenna Arrays

表 6 60 GHz 天线阵的关键参数比较

Parameters	Proposed antenna	[5]	[11]
Antenna type	Cavity-backed patch antenna	Slot antenna	Patch antenna
Process	Surface micro-machine	SIW	PCB

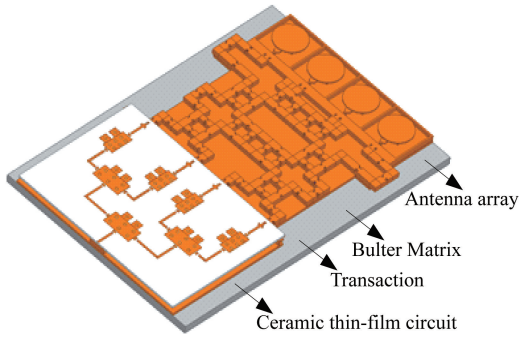

Fig. 13 A beam-steering antenna array

图 13 波束扫描天线阵

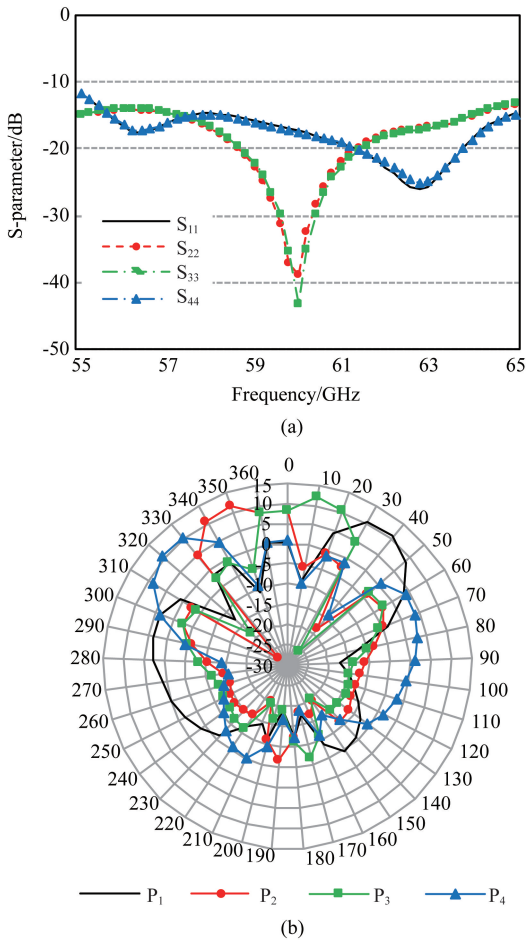

Fig. 14 Simulated performance of beam-steering antenna array. (a) S-parameter, (b) radiation pattern at 60 GHz

图 14 波束扫描天线的仿真性能 (a) S 参数, (b) 60 GHz 方向图

Parameters	Proposed antenna	[5]	[11]
Size (mm^3)	17.5×14.5×0.42	30×100×0.508	20×30×0.508
Bandwidth (GHz)	10 (55~65)	2.3 (58.5~60.7)	7 (57~64)
Gain (dBi)	11.8~12.1	11~13.5	11.6~12.3
Scanning beam	±11°, ±35°	±15°, ±42°	±35°, ±15°
The insertion loss of feed network	0.8	1.4	2

(下转第 580 页)

[10] Piquette E C, Edwall D D, Lee D L, *et al*. Precise arsenic doping of HgCdTe by MBE and effects on compositional interdiffusion[J]. *Journal of electronic materials*, 2006, **35**(6):1346-1349.
[11] Lee T S, Garland J, Grein C H, *et al*. Correlation of arsenic incorporation and its electrical activation in MBE HgCdTe[J]. *Journal of Electronic Materials*, 2000, **29**(6):869-872.
[12] Chen A C, Zandian M, Edwall D D, *et al*. MBE growth and characterization of in situ arsenic doped HgCdTe[J]. *Journal of electronic materials*, 1998, **27**(6):595-599.
[13] Pultz G N, Norton P W, Krueger E E, *et al*. Growth and characterization of P-on-n HgCdTe liquid-phase epitaxy heterojunction material for 11-18 μm applications[J]. *Journal of Vacuum Science & Technology B*, 1991, **9**(3):1724-1730.
[14] Arias J M, Pasko J G, Zandian M, *et al*. Planar p-on-n HgCdTe heterostructure photovoltaic detectors[J]. *Applied physics letters*, 1993, **62**(9):976-978.
[15] Maxey C D, Ahmed M U, Capper P, *et al*. Investigation of parameters to obtain reduced Shockley-Read traps and near radiatively limited lifetimes in MOVPE-grown MCT[J]. *Journal of Materials Science*: Materials in Electronics, 2000, 11(7): 565-568.
[16] Maxey C D, Fitzmaurice J C, Lau H W, *et al*. Current status of large-area MOVPE growth of HgCdTe device heterostructures for infrared focal plane arrays[J]. *Journal of electronic materials*, 2006, **35**(6):1275-1282.

(上接第568页)

4 Conclusions

Low loss rectangular micro-coaxial transmission line and beam-steering antenna array were designed and analyzed by surface micro-machined process in this paper. The rectangular micro-coaxial transmission line filled air substrate was fabricated and measured to achieve insertion loss less than 0.18 dB. The proposed beam-steering antenna array was proposed in an area of $17.5 \times 14.5 \times 0.42$ mm^3 and the wideband characteristics was obtained by ladder probe from 55 ~ 65 GHz, which includes worldwide unlicensed 60 GHz band. The proposed antenna array has wide beam steering capability covering 70° areas with 12.1 dBi gain for wireless terminals. Thus, the realized beam-steering antenna array is very suitable for low-cost 60 GHz short-rang indoor communication.

References

[1] Doan C, Emami S, Sobel D, *et al*. Design considerations for 60 GHz CMOS radios[J]. *IEEE Communications Magazine*, 2014, **42**(12): 132-140.
[2] Baek Y H, Truong L H. Park S W, *et al*. 94 GHz log-periodic antenna on GaAs substrate using air-bridge structure[J]. *IEEE Antennas Wireless and Propagation Letter*, 2009, **8**:909-911.
[3] Perrot S, Person C, Qwndo C, *et al*. Low cost millimeter wave aperture coupled antenna array on polymer membrane substrate[C]. *IEEE MTT-S International Microwave Symposium Digest*, 2000: 577-580.
[4] Fan Fan He, Ke Wu, Wei Hong, *et al*. Low-cost 60 GHz smart antenna receiver subsystem based on substrate integrated waveguide technology[J]. *IEEE Transactions on Microwave Theory and Techniques*, 2012, **60**(4):1-10.
[5] Tian Y, Lee K, Wang H. Air-gapped microcoxial transmission line for ultrawide band microwave and millimeter wave ICs[J]. *Microwave and Optical Technology Letter*, 2014, **56**(6):1462-1465.
[6] Lee J, Hong S, Kim W, *et al*. A switched array antenna module for millimeter-wave wireless communications[C]. *Global Symposium on Millimeter Waves*, 2008:161-163.
[7] Costa J, Lima E, Fernandes C. Compact beam-steerable lens antenna for 60 GHz wireless communications[J]. *IEEE Transactions on Antennas and Propagation*, 2009, **57**(9):2926-2933.
[8] William F, Moulder, Waleed Khalil, John L. Volakis. 60 GHz Two-dimensionally scanning array employing wideband planar switched beam network[J], *IEEE Antennas and Wireless Propagation Letter*, 2010, **9**:818-821.
[9] Ismail Ben Mabrouk, Julien Hautcoeur, Larbi Talbi, *et al*. Feasibility of a millimeter-wave MIMO system for short-range wireless communications in an underground gold mine[J]. *IEEE Transactions on Antennas and Propagation*, 2013, **61**(8):4296-4305.
[10] Reid J Robert , Eric D Marsh, Richard T Webster. Micromachined rectangular-coaxial transmission line[J]. *IEEE Transactions on Microwave Theory and Techniques*, 2006, **35**(1):3433-3442.
[11] Chen T S. Determination of the capacitance, inductance and characteristic impedance of rectangular lines[J]. IEEE *Transactions on Microwave Theory and Techniques*, 1960, **8**(5):510-519.
[12] Yang Tian, Nan Li, Hong Wang, *et al*. Right-Angled microcoaxial bends for Si-based RF/microwave integrated circuits[J]. *IEEE Transcations on Components*, Packaging and Manufacturing Technology, 2016, **6**(2):290-297.